Chalcogenide Letters Vol. 21, No. 11, November 2024, p. 867 - 872

Influence of growth temperature on the structural and optical characteristics of PbZnS thin films

M. Temiz [a,*], S Çelik [b]
[a] *University of Selcuk Karapınar Aydoganlar Vocational School, 42400 Konya, Turkey*
[b] *University of Gaziantep Engineering Facuty 27200 Gaziantep, Turkey*

Ternary thin films have garnered significant attention due to their adjustable band gap characteristics, making them suitable for many applications. In this research, we examined the structural and optical characteristics of PbZnS thin films fabricated onto glass substrates employing the spray pyrolysis techniuqe. The films were fabricated at different temperatures ranging from 300 to 400°C. X-ray diffraction (XRD) analysis indicated that all films displayed a cubic structure with a preferred orientation along the (200) plane. From the analysis of XRD peaks, it was observed that the crystal structure initially improved with increasing temperature but then began to degrade. These films demonstrated strong absorption in the range of 350–1600 nm. The optical bandgap (Eg) values, calculated based on the relationship between the absorption coefficient and photon energy, showed slight variations around 2 eV. Notably, the band gap decreased with growth temperatures up to 350°C, then increased at higher temperatures. These fluctuations are attributed to factors such as thermal expansion, strain, defects, surface/interface effects, and changes in doping or composition.

(Received July 9, 2024; Accepted November 4, 2024)

Keywords: PbZnS thin films, Growth temperature, Structural properties, Optical properties, Spray pyrolysis, Band gap energy

1. Introduction

From a materials science standpoint, compound semiconductors have long been a focal point due to their exceptional electronic and optical properties[1]. These semiconductors are utilized in a wide range of electronic applications, including optical converters, photoconductors, optical sensors, field-effect transistors, and solar cells [2, 3]. Moreover, PbZnS thin films hold potential for use in various electronic equipments like photoconductors, light-emitting diodes, solar cells, field-effect transistors, and sensors [4–6]. PbZnS thin films can be synthesized through multiple techniques, including chemical bath deposition, spray pyrolysis, sol-gel, sequential ionic layer adsorption and reaction (SILAR), sputtering, pulsed laser deposition, and electron beam evaporation, all of which are commonly employed methods [7].

In this research, the effects of growth temperature on the structural and optical features of PbZnS films were explored. The films were produced using the chemical spray pyrolysis technique. This method was selected for its simplicity, cost-effectiveness, and time efficiency, making it an accessible and efficient option for thin film fabrication.

2. Experimental procedure

The chemical spray pyrolysis method was employed to produce PbZnS thin films. The chemicals utilized for the fabrication process were lead acetate Pb(CH3CO2)2, thiourea (CS(NH2)2), and zinc acetate dihydrate Zn(CH3COO)2.2(H2O). To prepare the solution, 0.1 M of lead acetate, thiourea, and zinc acetate dihydrate were dissolved in 50 ml of water. The mixture was

* Corresponding author: mehmettemiz@selcuk.edu.tr
https://doi.org/10.15251/CL.2024.2111.867

mixed for 30 minutes employing a magnetic mixer to ensure thorough homogenization. The resulting solution was atomized onto glass substrates at varying temperatures of 300, 325, 350, 375, and 400°C employing the spray pyrolysis method. X-ray diffraction data for the PbZnS thin films were obtained using a high-resolution X-ray diffractometer (Model: Rigaku D/MAX/-220) equipped with CuKα radiation (λ=1.5406 Å) as the X-ray source.

3. Results and discussion

3.1. Structural properties

The XRD patterns of PbZnS thin films growth at different substrate temperatures (300, 325, 350, 375, and 400) are shown in Figure 1. When we examine the XRD data, we see the presence of more than one peak. This gives us the idea that PbZnS films have a polycrystalline structure. It can be seen that the X-ray diffraction spectrum of all films have distinct peaks in the (1 1 1) and (2 0 0) planes, while the (2 2 0), (3 1 1) and (2 2 2) planes have small peaks according to JCPDC Card no. 65-0692.

The interplanar spacing (d) is calculated with the equations given below.

$$2dsin\Theta = n\lambda \tag{1}$$

where Θ is the Bragg angle and λ is the wavelength of X-ray.

Employing the equation given above, the lattice parameter for the cubic phase is calculated as follows[8].

$$a = d_{hkl}\sqrt{h^2 + k^2 + l^2} \tag{2}$$

We calculated the lattice parameters for the films grown at different base temperatures using the corresponding formula and plotted them in figure 1.

The Scherrer formula we use to determine the crystal grain size (t) of films is given as follows[9]:

$$t = \frac{0{,}9\lambda}{\beta Cos\theta} \tag{3}$$

where β, λ, and θ are FWHM of the peak, the 1.5406 Å wavelength of the X-ray, and their peak position, respectively.

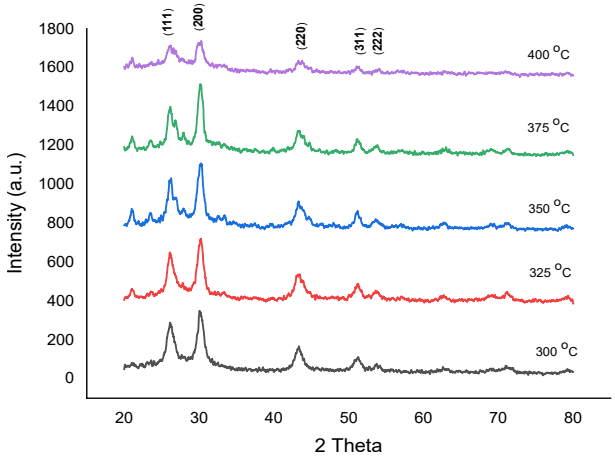

Fig. 1. XRD patterns of PbZnS thin films with different growth temperatures.

Figure 1 presents the XRD patterns of PbZnS films fabricated at different substrate temperatures. The results indicate that the crystal structure experiences some disruption. All films exhibit a prominent peak corresponding to the (200) plane, which aligns with the cubic structure of PbS, having lattice parameters of a = 0.59143 nm [10]. Additionally, minor peaks associated with the (111), (220), (311), and (222) planes are observed at 26.10°, 43.22°, 51.20°, and 53.6°, respectively. These findings are consistent with the PDF number (78–1054) from the reference database.

Table 1. The 2θ values, distance between planes, lattice constant, grain size and micro strain of PbZnS films with different growth temperatures.

Growth temperature (^{0}C)	2 Θ Value (^{0})	Inter- Planner d (A^0)	Lattice Constant A^0	Grain size (nm)	Microstrain
300	30,17	2,9598	5,9196	23,98	0,001445
325	30,29	2,9483	5,8966	31,08	0,001116
350	30,19	2,9579	5,9158	42,01	0,0008274
375	30,18	2,9588	5,9176	19,25	0,001550
400	30,15	2,9617	5,9234	14,75	0,002351

When Figure 1 and Table 1 are examined in detail, it is noted that the XRD patterns of the PbZnS thin films we produced show an increase in peak intensities and grain sizes as the substrate temperature increases up to 350 degrees. However, beyond this temperature, at 375 and 400 degrees, the peaks begin to deteriorate, and the grain sizes start to decrease.

Decrease from 300 °C to 350 °C: A continuous decrease in the microstrain value is observed as the temperature decreases from 300 °C to 350 °C. This can be interpreted as a decrease in the stress in the crystal arrangement of the material and an increase in the regularity of the crystal structure. In this temperature range, crystal growth and rearrangement can cause the strains to decrease.

Increase after 350 °C: An evident increase in the microstrain value is noted as the temperature rises beyond 350 °C to 375 °C and 400 °C. This increase indicates that the crystalline structure of the material has started to deteriorate, and the stresses increase with increasing temperature. At 375 °C and 400 °C, the increase of irregularities and dislocations in the crystal structure can increase the microstrain values.

In general, in the production of PbZnS thin films, temperature increases up to 350 °C make the crystal structure more regular, while increases beyond this temperature increase the distortions in the crystal structure and increase the strains. Therefore, 350 °C can be considered as an optimum temperature

There may be various reasons for this situation as follows:

Thermal Stress and Strain: Higher growth temperatures can cause significant thermal stress in films. As temperature increases, the mismatch in thermal expansion coefficients between the film and the substrate begins to increase, resulting in increased strain[11].

Inhibition of Grain Growth: With the increase in energy due to high temperatures, nucleation rates increase but grain growth rates decrease. These results are seen in smaller grains because the greater number of nucleation points limits the size of each grain that can be obtained before it meets neighboring grain[12].

Defect Formation: At higher temperatures, an increase in the formation of defects and dislocations within the crystal structure can be observed. These defects cause a disruption in the periodicity of the crystal lattice and can lead to broader and less intense XRD peaks[13].

The combination of a reducing in grain size and an rising in defects can cause distortion of XRD peaks. Smaller grains have more grain boundaries, which can scatter X-rays more diffusely, leading to a decrease in peak intensity and clarity[14].

3.2. Optical properties

To examine the optical properties of PbS films, optical absorbance observations of PbZnS films were carried out across the wavelength spectrum of 300–1000 nm at room temperature with normal incidence. Figure 2 presents the absorption spectra of the PbZnS thin films. All the films display similar absorption edges. It is evident that PbZnS films exhibit high absorption within the wavelength spectrum of 350–1600 nm. The film grown at 300°C shows a significant decrease in absorbance beyond 800 nm, a trend that is not observed in the films grown at other temperatures.

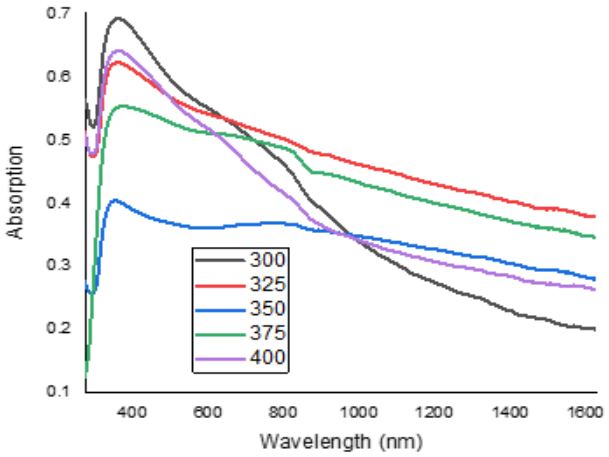

Fig. 2. Absorption spectra of the PbZnS thin films with different growth temperatures.

The optical bandgaps (Eg) of the films were determined employing the relationship among the absorption parameter (α) and the photonic energy (hυ). This relationship is described by the following equation[15]:

$$(\alpha h\vartheta) = A(h\vartheta - E_g)^{1/2} \quad (4)$$

Here, A is a constant related to the effective masses. The bandgap values were computed by drawing $(\alpha h\upsilon)^2$ against hυ and extrapolating the linear portion of the plot to the energy axis where α=0 (Figure 2). The optical bandgap energy of the films exhibited slight variations, staying around 2 eV, which aligns well with the literature [16]. However, as the growth temperature increased, the bandgap decreased up to 350°C, followed by an increase at 375°C and 400°C

The behavior of the band gap with increasing growth temperature in thin semiconductor films can be explained by considering several factors related to the film's structure and properties:

Thermal Expansion and Lattice Constant: As the growth temperature rises, the system gains more thermal energy, causing the lattice to expand. This thermal expansion can result in a reduction of the effective lattice constant in the film. Typically, as the lattice constant increases, the bandgap energy decreases. This occurs because the bond strength between atoms weakens, resulting in a narrower energy gap.

Strain and Defects: Changes in growth temperature can affect the strain and defect density within the film. At temperatures below 350°C, the decrease in band gap might be due to strain relaxation and reduction in defect density, which can lead to a more perfect crystal structure.At higher temperatures (375°C and 400°C), the increase in band gap may indicate an increase in defect density or strain due to the film becoming more disordered or mismatched with the substrate.

Surface and Interface Effects: Growth temperature affects the surface and interface quality of the film. Lower temperatures might lead to smoother interfaces and fewer surface states, whereas higher temperatures can increase surface roughness and the number of interface states, affecting the band structure[17].

Doping and Composition Changes:Growth temperature can influence the doping and composition of the film. Changes in these parameters can affect the band structure and band gap energy[18].

In summary, the observed changes in the band gap with growth temperature are likely due to a combination of strain relaxation, defects, changes in lattice constant, surface/interface effects, quantum confinement, and changes in doping or composition.

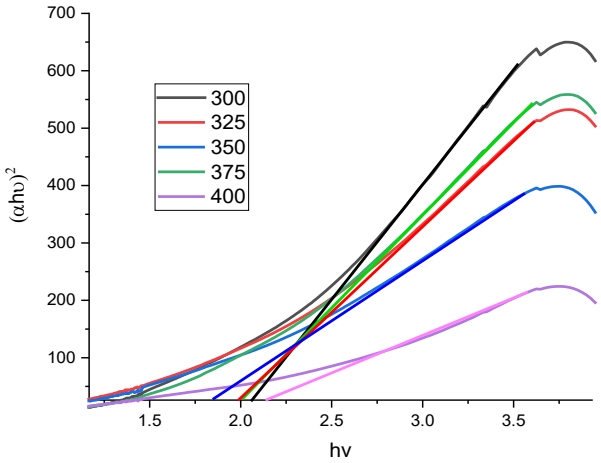

Fig. 3. Graphs of (αhv)2 vs. hv of the PbZnS films with different growth temperatures.

4.Conclusion

In conclusion, this research underscores the substantial effect that growth temperature has on the physical characteristics of PbZnS thin films.The findings offer important insights for optimizing growth conditions to achieve specific structural and optical characteristics for applications like solar cells, light-emitting diodes, and sensors. Future research could delve deeper into the mechanisms driving these temperature-induced variations and explore other growth parameters to further improve the performance of PbZnS thin films in electronic and optoelectronic devices.

References

[1] Y. Vasudeva Reddy, M. Kumar T, T. Shekharam, M. Nagabhushanam, Int. J. Eng. Sci. Invent. 7(1), 2319 (2018).

[2] M. L. Madugu, O. I. O. Olusola, O. K. Echendu, et al., J. Electron. Mater. 45(10), 2710 (2016); https://doi.org/10.1007/s11664-015-4310-7

[3] S. Ravishankar, A. R. Balu, J. Mater. Sci. Mater. Electron. 33(3), 506 (2017); https://doi.org/10.1080/02670844.2016.1267832

[4] J. Han, G. Fu, V. Krishnakumar, et al., J. Phys. Chem. Solids 74(11), 1879 (2013); https://doi.org/10.1016/j.jpcs.2013.08.004

[5] O. K. Echendu, I. M. Dharmadasa, J. Electron. Mater. 43(4), 791 (2014); https://doi.org/10.1007/s11664-013-2943-y

[6] O. K. Echendu, I. M. Dharmadasa, Energies 8(5), 4416 (2015); https://doi.org/10.3390/en8054416

[7] H. Ates, E. Bahceci, Nano Malzemeler için Üretim Yöntemleri, Gazi Üniversitesi Fen Bilim Dergisi, 492 (2015).

[8] B. D. Cullity, Elements of X-ray Diffraction, Addison-Wesley Publishing Company, Inc, 187 (1978).

[9] L. S. Birks, H. Friedman, J. Appl. Phys. 17(6), 687 (1946); https://doi.org/10.1063/1.1707771

[10] B. Abdallah, R. Hussein, N. Al-Kafri, W. Zetoun, Iran J. Sci. Technol. Trans. A Sci. 43(7), 1371 (2019); https://doi.org/10.1007/s40995-019-00698-1

[11] K. N. Tu, Electron Thin-Film Reliab. 118 (2010).

[12] F. Najafkhani, S. Kheiri, B. Pourbahari, H. Mirzadeh, Arch. Civ. Mech. Eng. 21(1), 1 (2021); https://doi.org/10.1007/s43452-021-00185-8

[13] S. Dolabella, A. Borzì, A. Dommann, A. Neels, Small Methods 6(3), 1 (2022); https://doi.org/10.1002/smtd.202100932

[14] M. Shafi P, C. Bose A, AIP Adv. 5(4), 1 (2015).

[15] S. Ravishankar, A. R. Balu, M. Anbarasi, V. S. Nagarethinam, Optik (Stuttg) 126(9), 2550 (2015); https://doi.org/10.1016/j.ijleo.2015.06.039

[16] D. Saikia, P. Phukan, Thin Solid Films 562(5), 239 (2014); https://doi.org/10.1016/j.tsf.2014.04.065

[17] L. A. Cipriano, G. Di Liberto, S. Tosoni, G. Pacchioni, Nanoscale 12(8), 17494 (2020); https://doi.org/10.1039/D0NR03577G

[18] Z. Jiang, A. Hoffmann, A. Schleife, Phys. Rev. B 1(1), 1 (2024).